SHIP VISCOUS FLOW
A REPORT ON THE 1990 SSPA-CTH-IIHR Workshop

Virendra C. Patel
Iowa Institute of Hydraulic Research
Iowa City, Iowa

Lars Larsson
Chalmers University of Technology and
FLOWTECH International AB
Gothenburg, Sweden

Abstract

To assess the state of the art in ship viscous flow computation a Workshop was organized in 1990 by three organizations: SSPA Maritime Consulting AB, Chalmers University of Technology and Iowa Institute of Hydraulic Research. Two test cases were specified by the organizers and sent out to all interested research groups, which were asked to submit results in a prescribed format. In Septemer 1990 a meeting was held at Chalmers University of Technology. All results had then been collected and presented in a common format, and the theories behind the methods compiled in a table based on responses to a questionnaire sent our earlier. During the meeting, each research group was first given the opportunity to briefly introduce their method and results. Thereafter, a considerable time was spent on general discussions on the performance of the different methods considering the differences in the underlying theories. Specific items that were adressed were grid generation, governing equations, boundary conditions, turbulence modelling and numerical method. Practical aspects on the results, for instance from the point of view of propeller design, were also discussed. The Workshop Proceedings contain a description of the participating methods and the results of both test cases. In the present paper a summary of the Workshop and its results is presented.

Introduction

Although viscosity is present in the entire flow around a ship it has a significant effect only in the boundary layer around the ship and the wake behind it. The present paper deals with the flow in these two regions, which are limited in size, but very important from at least two points of view. Frictional forces within the boundary layer give rise to a viscous resistance of the ship, in most cases the dominant resistance component, and the velocity distribution in the near wake determines the design and performance of the propeller.

Despite its obvious importance the first serious attempts to compute the viscous flow were made relatively recently, about twenty years ago. This is in contrast to the long term research in the inviscid flow area, where wave resistance research has been under way during the entire twentieth century. The reason for the difference is that the complicated viscous flow equations, i.e. the Navier-Stokes equations and approximations thereof, are less amenable to analytical treatment than the inviscid equations, normally based on potential flow theory. Therefore it was not until computers had become powerful enough to handle three-dimensional boundary layer theory numerically that research on viscous flow computations was started.

During the 1970's a number of methods for predicting ship boundary layers were developed, and in 1980 it was considered appropriate to assess the state of the art in this area. To accomplish this, an international Workshop on ship boundary layers was organized by SSPA, the Swedish State Shipbuilding Experimental Tank, in cooperation with the International Towing Tank Conference, ITTC[1]. The purpose was to bring together specialists on ship boundary layer calculations from all over the world, and to let them apply their techniques and methods to two test cases, specified in detail by the organizers. In June of 1980 a meeting was held in Gothenburg. The results of 17 methods had then been collected and presented in a uniform format. During the meeting the various components of the methods were discussed in the light of the results produced. The general finding was that most methods were able to predict the thin boundary layer over the major part of the hull with an accuracy sufficient for engineering purposes, while all of the methods failed completely in predicting the flow near the stern and in the wake.

In the 1980's development accelerated, and the focus was changed from the thin boundary layer to the stern/wake flow. As evidenced by the 1980 Workshop a new class of methods with less restrictive approximations was required. The interest of researchers was soon focused on the Reynolds Averaged Navier-Stokes (RANS) equations, and a number of such methods was proposed during the 1980's. Towards the end of the decade it was considered timely to organize a second Workshop to investigate the progress made. This task was undertaken by three organizations: SSPA Maritime Consulting and Chalmers University of Technology (CTH) in Sweden and Iowa Institute of Hydraulic Research (IIHR) in the USA.

As in the first Workshop, the purpose of the new event was twofold:

- to assess the state of the art in ship viscous flow calculations
- to analyze the results of the different methods in light of the underlying theories, thereby obtaining information on the most promising ways to achieve further improvement

The 1980 Workshop had been successful in achieving these goals, so the new Workshop was organized in a similar way. Two test cases were selected. The so-called HSVA tanker[2] was again chosen, as being the best documented test case available, see for instance Hoffmann[3] and Wieghardt and Kux[4]. Even though measurement data have been obtained only at model Reynolds numbers, the participants were asked, as an optional exercise, to carry out calculations also for a full scale Reynolds number. This was to shed some light on the difficulties encountered at this larger scale, for which calculations have been very rare, so far. The second test case was designed to produce a significantly different stern flow with a minimum change of geometry . More information about the design philosophy is given in the next section. A very important feature of the second case (the "Mystery case") was that no measurement data were available when the calculations were carried out.

As in the first Workshop, attention was confined to double models, in which wave effects are absent and the free surface may be considered as a plane of symmetry. Also, only the flow on the bare hull, without appendages and propulsors, was considered.

The first announcement of the "1990 SSPA-CTH-IIHR Workshop on Ship Viscous Flow" was distributed in late 1988, together with a questionnaire to be returned by 15 May 1989 by all researchers interested in taking part in the Workshop calculations. Efforts were made to invite participation by originators of commercial CFD codes. No less than 21 computors indicated their interest in participating, and in August the data and instructions for the first test case were sent out. Similar information for the second case was distributed in December. In the early summer of 1990 results from 19 methods had been received. and the difficult task of condensing all the information into a uniform format was started at CTH. By the time of the Workshop meeting, which was held at CTH 12-14 September 1990, all results had been plotted in a way such that comparison between the different methods could be easily made. Further, the replies to the questionnaire had been compiled at IIHR and condensed into a table, useful for quick reference to the theory behind each method.

In the present paper a brief summary of the Workshop is given. The two test cases are described next, followed by an overview of the methods. Thereafter, some important results are discussed and finally some conclusions are drawn. For a full account of the Workshop, reference should be made to the Proceedings[5].

Test cases

HSVA Tanker, Case I

A body plan of the first test case, the HSVA tanker is shown in Fig. 1. The boundary layer measurements by Hoffmann[3], and the subsequent stern-flow measurements by Wieghardt, Kux and Knaack[4], were made on a double model of this hull in a 1.2 m diameter, slotted-wall wind tunnel, in which the turbulence level was of the order of 1 percent. Different types of pressure probes were used. The model was supported in the tunnel by means of wires and a sting at the stern. The nominal length of the model was 2.74 m but for reference length we have used the length between perpendiculars, L = 2.664 m, which gives a Reynolds number of $5 \cdot 10^6$. Neither the tunnel nor the support were modeled by any of the computors.

Mystery hull, Case II

The second test case, for which no measured data were available by the time of the meeting, was designed by Prof G. Dyne at Chalmers and Mr L.G. Jonsson at SSPA. The purpose was to create a significantly different wake pattern with a minimum of geometry change as compared to the first case. Thus, only the stern sections were modified. By making them more U-shaped stronger longitudinal vortices could be expected behind the hull, creating a more distorted wake field, see Dyne[6]. A body plan is shown in Fig. 2.

Velocity measurements using Laser-Doppler Velocimetry were carried out at the University of Hamburg after the Workshop[7], but the results are analyzed and included in the Proceedings[5].

Overview of methods

Some 19 organizations from 12 countries participated in the Workshop. A summary of the important characteristics of the methods is presented in Table 1 (at the end of the paper). This table was prepared on the basis of information supplied by the participants in a questionnaire that was distributed at the beginning and again at the end of the Workshop. Effort was made to obtain as much and as accurate information as possible on each method. The following is a review of some of the similarities and differences among the methods.

The overall strategy summarized in item A indicates that 12 participants restricted their calculations to the stern and wake flow (S) while 7 treated the complete hull (H), including the bow. Both global (G) and zonal (Z) methods are represented but the most common combination is a global method applied to the stern flow (S,G). The 5 zonal approaches employ an inviscid-flow method. In three of these,

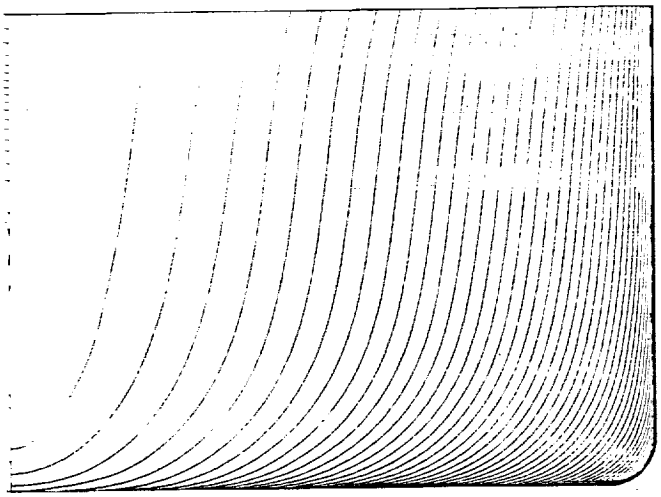

Forebody

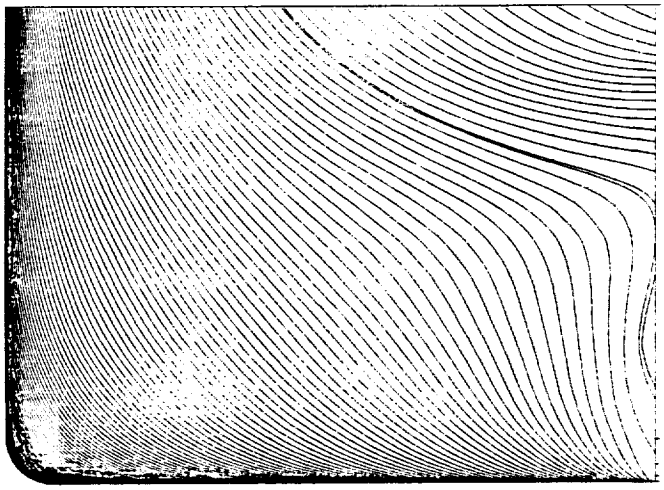

Afterbody

1. Body plan, HSVA Tanker

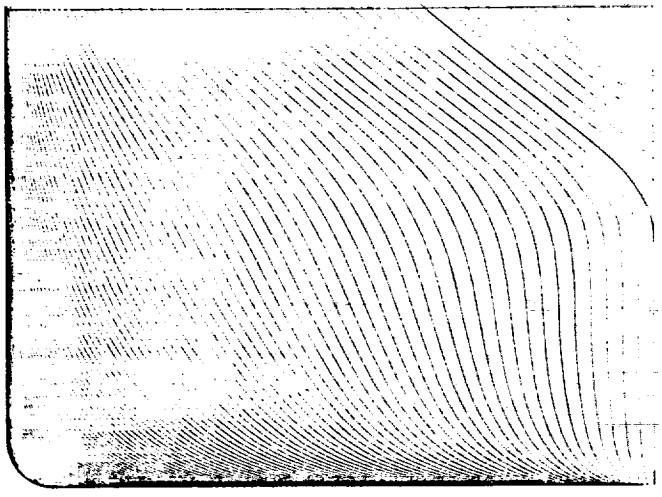

2. Body plan, Mystery Hull (Forebody as HSVA Tanker)

the viscous and inviscid solutions are matched at a specified boundary outside the viscous layer. One participant group (CT) made both global and zonal calculations. However, only the results from their global calculations are presented here. It is significant to note that none of the zonal approaches performed iterations between the viscous and inviscid flows to allow for interaction although in some cases the match boundary between the two zones was placed rather close to the hull.

Section B of Table 1 summarizes the equations and variables. One method employs integral equations and therefore provides a link to the earlier ship boundary layer Workshop[1]. It is clear that much of the information sought through the questionnaire is not relevant to the integral approach and therefore there are very few entries for that method. Among the differential methods, a vast majority solves the Reynolds-Averaged Navier-Stokes equations, while four adopt reduced forms (P, Ra) of these equations. One method uses large-eddy simulation along with a subgrid turbulence model. In all cases, the equations are solved in the so-called primitive variables, i.e., velocity and pressure. Thus, for example, methods that use vorticity or stream functions are not represented. There is a great deal of variability in the choice of the velocity components, ranging from simple, orthogonal ones to covariant components and grid-oriented nonorthogonal components. This choice impacts on the complexity of the codes and storage requirements for the geometrical quantities associated with the grid. Most methods employ nonorthogonal coordinates in all planes, but a few retain orthogonality in one (usually transverse) plane. This particular feature is related to the manner in which the grid is generated.

With the exception of the integral approach, all methods require a model for turbulence. These are summarized in section C. It is seen that 4 methods use algebraic models of eddy viscosity or mixing length (AL) and 13 employ the k-ϵ model. The large-eddy simulation method uses the Smagorinsky eddy-viscosity model along with the van Driest damping function for the subgrid scales. Of the 4 methods that employ algebraic, zero-equation models, three use the Baldwin-Lomax model and one (H) uses the mixing-length model. As far as can be ascertained, all users of the two-equation k-ϵ model retain the same constants, (C_μ, $C_{\mu 1}$, $C_{\mu 2}$, G_k, G_ϵ) = (0.09, 1.44, 1.92, 1.0, 1.3). In two cases (HC, PV), however, the basic k-ϵ model is combined with a one-equation model for the near-wall region, while others employ the wall function approach. These two, and the methods employing algebraic models, integrate the flow equations up to the wall, where the no-slip condition is applied. This approach requires many more grid points in the near-wall region to resolve the large gradients of velocity and eddy viscosity. Methods using the wall-function approach,

on the other hand, satisfy the law of the wall and related conditions at one or more grid points away from the wall, and do not explicitly solve the flow equations in the near-wall layer.

Section D of Table 1 provides an overview of the boundary and initial conditions employed in the various calculations. As all methods approach the solution either by a time marching or an iterative process, all require initial conditions (time = 0). In this respect, three methods start the solution from rest, 7 use uniform flow, one uses boundary layer solutions, another uses a potential flow solution, while 5 indicate some other procedure. Among the last category are methods in which a parabolic march is made through the solution domain with an assumed initial pressure field. There is also considerable variation among methods in the quantities that are determined or prescribed at the start of the calculations. The initial conditions presumably influence the number of iterations or time steps required to obtain the steady state solutions that are sought.

The upstream boundary conditions depend upon whether the solution is obtained for the entire hull or only the stern and wake flow. In the case of the calculations for the entire hull, two types of treatment have been made. In five of the seven such calculations, the upstream boundary is placed about one-half ship length ahead of the bow, and quite simple boundary conditions are prescribed in the uniform flow there. In the remaining two (IL and KaO), the boundary layer over the bow is calculated. It appears that none of these calculations takes any account of the initial region of laminar flow or of the transition that was provoked artificially in the experiments. In the 12 calculations that were restricted to the stern and wake flow, there are differences in the location where the calculations were started as well as in the parameters that are prescribed. Three participants started the calculations at a check station, X/L = 0.646, where the integral parameters of the boundary layer were supplied from experiment. (The X-axis is along the hull, with the origin at the bow.) Others started the calculations somewhat ahead of this section, using, in some cases, the data at the check station as a guide. In all such calculations, however, the detailed velocity and turbulence parameter distributions required by the methods had to be generated by the participants. In this regard, most appear to have used two-dimensional boundary layer correlations, with the three dimensionality neglected. In one case (PJL), however, a special updating scheme was devised to obtain a set of initial conditions that is consistent with the equations being solved. The differences in the initial conditions are likely to be observed most clearly in the results at the check station.

There is also considerable variation in the location of the downstream boundary where the solutions terminate, and the conditions applied at that boundary. In most cases the solutions are taken far enough from the stern to assume a negligible upstream influence and for the parabolic or extrapolated conditions to be valid.

The boundary conditions at the hull surface were discussed above in connection with the turbulence model. For completeness, however, we note that the no-slip conditions are applied explicitly in some methods whereas they are satisfied indirectly in methods that rely on the wall-functions approach.

All of the calculations presented at the Workshop have exploited the geometric symmetry about the ship centerplane and calculated only one half of the hull. Also, all participants assumed a double body and applied symmetry conditions along the water plane.

The location of the solution boundary in the "farfield" some distance from the ship axis, and the conditions specified along that boundary, also show considerable differences. With respect to the location, the five zonal calculations performed with viscous and inviscid methods use a boundary that varies from 0.08 of a ship length in one case (H) to 0.7 in another (KaO). Recall that this is the boundary at which the two solutions are matched and, as noted earlier, none of the calculations accounted for the interactions between the two regions. In these zonal calculations, the inviscid solutions provided the boundary conditions for the viscous solutions. In the remaining, global approaches, the location of the farfield boundary ranged from 0.1 of a ship length (T) to 1.5 (HC) with many using a value of one ship length. However, those who have used boundaries rather close to the hull (SZC and T) have provided boundary conditions from inviscid flow. In this respect, these methods, characterised as global by their originators, could also be regarded as zonal. Methods that have placed the boundary at larger distances from the hull have tended to prescribe uniform-flow conditions in the far field. Some differences are observed, however, in these cases in the particular variables or conditions that are specified or satisfied; see, for example, codes C and A in the table.

Section E of Table 1 pertains to the generation and control of the numerical grid. For the Workshop calculations, all participants employed a single block grid although one (GCHM) indicated that their method can accommodate a multi-block grid. Fully nonorthogonal grids as well as grids that are orthogonal in some planes (typically in the transverse sections) or at boundaries (usually at the hull) are represented in the calculations. The most popular method for generating the grid appears to be numerical, although some participants have employed analytic and algebraic methods, and even combinations of methods.

Among the numerical approaches, elliptic methods for the entire three-dimensional solution domain are the most common. Several methods use post-generation smoothing of the grid. Control of the grid is exercised most commonly from the boundaries although some indicate that it is done from inside the solution domain.

The numerical features of the various methods are summarized in section F. First of all, we note that there is no participation from the finite-element community and therefore items in the questionnaire that were designed specifically to obtain information on such methods are deleted in the table. Of the methods represented at the Workshop, there are four finite-difference methods, 10 finite-volume methods, and, for lack of a better term, four are classified as mixed methods. To these must be added the one based on integral equations which are also solved by finite-difference methods. It should be pointed out that not all of the methods in each of these categories are generically different. In other words, there are groups of methods in each class which share a great deal in common and, from a numerical perspective, may be classified as a single method. Be that as it may, we shall note the most significant features of the methods represented here.

First, discretization in both staggered and regular (colocated) grids is used in finite-difference as well as finite-volume methods. There is some correlation between the type of grid used and the method employed to solve for the pressure (or establish the pressure-velocity coupling) for this incompressible flow. Differencing of the convective terms is made by a variety of means, including upwinding, central differences, hybrid combinations and use of analytic solutions (FA). The responses to the questions on formal order of accuracy and formally conserved quantities are rather surprising. Most methods claim first or second-order accuracy but two consider their methods to be accurate upto the third order. The response to the second question seems to be correlated with the equations that are solved rather than any formal attempt in the methods to conserve mass, momentum, and total energy.

For the pressure, four methods use fully-coupled solutions. Two of these (GCHM and K) employ artificial compressibility, one (AS) uses a discretized continuity equation, another (H) uses the normal momentum equation. Most of the remaining methods employ segregated pressure-velocity coupling algorithms, SIMPLE being the most common.

In the execution of the solutions, most methods employ iterative techniques with under-relaxation or variable time steps. Explicit as well as implicit methods are represented. The solutions of the discretized algebraic equations are obtained using different tactics, including point substitution, line substitution, LU decomposition of matrices, and ADI methods.

Section G of Table 1 concerns the computations performed by the participants. As the two test cases are not substantially different with respect to the computational effort involved, the numbers in this section are typical of both cases. First of all, it is quite significant that calculations have been performed not only on state-of-the-art supercomputers (designated by S) but also on smaller machines (designated by M), such as workstations. The total number of grid points employed shows a great deal of variation, ranging from a low of 8,000 to a high of 253,000. It is interesting to note that the higher numbers are not necessariliy correlated with the use of supercomputers, nor are they correlated with the use of near-wall turbulence models or calculations made for the entire hull including the bow.

The number of time steps or iterations performed to obtain the solutions presented here varied widely, ranging from only 40 (BZLS and SZC) to 20,000 (ZM), although, in the latter case, the large-eddy simulation should never realize a steady state as defined for the other methods. It should be noted that a variety of convergence criteria were adopted to declare that a steady state had been obtained. The storage requirements and computer run times also varied over very wide limits. This is not surprising in view of the differences in the number of grid points and machines employed, but it is interesting to note that run times ranging from several hours to 5 days were reported by users of the smaller machines. The differences in the machines are also reflected in the cpu time per iteration per grid point. The fastest times were of course reported by users of supercomputers.

Results and Discussion

Results were requested from the participants at a Reynolds number of $5 \cdot 10^6$ for both hulls. As an optional exercise the computors were also asked to submit full scale results corresponding to a Reynolds number of $2 \cdot 10^9$ for case I. All but one delivered the model scale predictions but only three had computed the high Reynolds number case.

Pressure and friction distributions were reported at the waterline and keel and along three section girths on the hull, while velocity distributions in the form of iso-velocity contours and, in some cases, cross-flow vectors were given at four sections. For the most interesting section, the propeller plane, the pressure and (if computed) the turbulent kinetic energy were also reported.

The complete results may be found in the Proceedings[5], but in the present paper only a few representative examples will be given. These include the pressure distribution along three section girths and the velocity distribution (iso-velocities and

Abdallah & Sotiropoulos

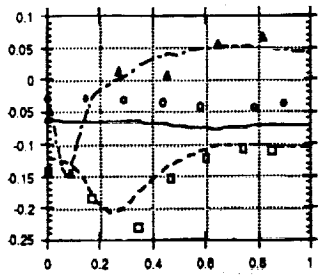

Broberg, Zhang, Larsson & Schöön

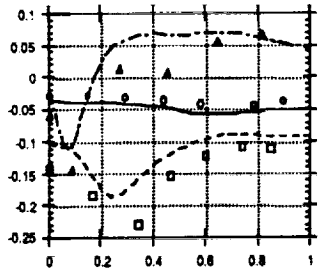

Bull, Watson & Musker

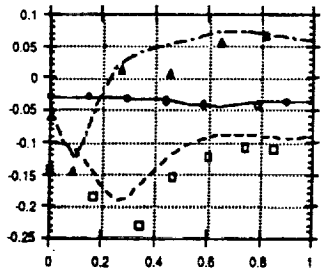

Caprino & Traverso

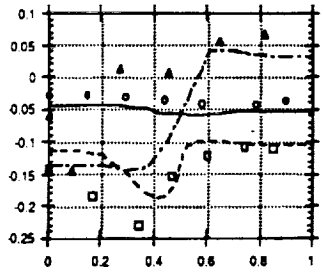

Gorski, Coleman, Haussling & Miller

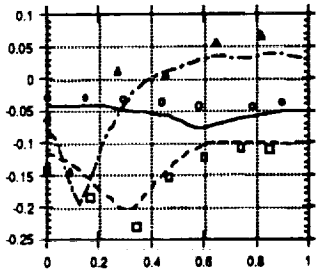

Hoekstra

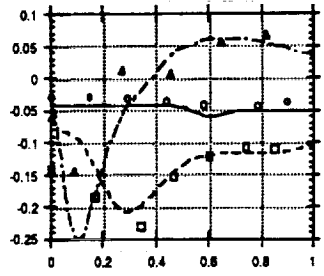

Hoffman &Chan

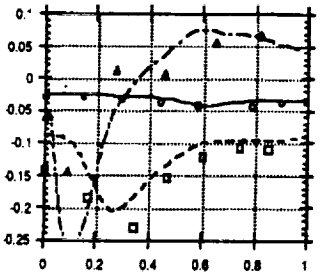

Ikehata & Liu

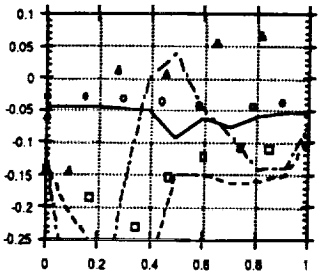

Kang & Oh

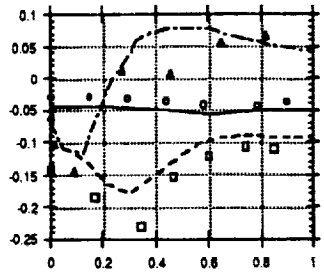

Kodama

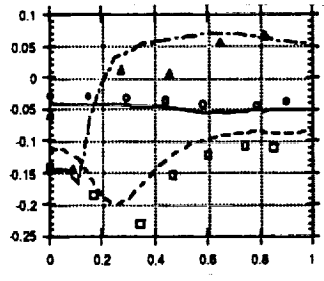

Kanevsky & Orlov

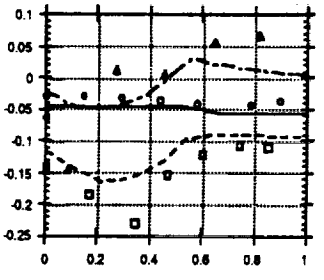

Majumdar, Zhu & Rodi

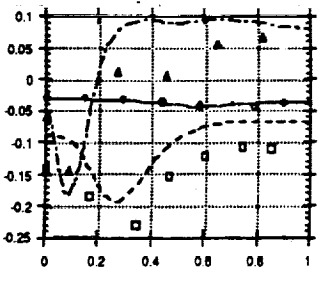

Masuko, Shirose & Abe

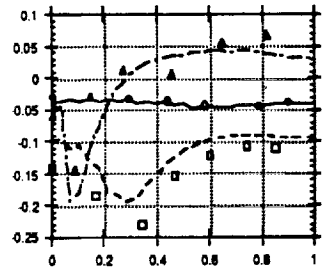

Patel, Ju & Lew

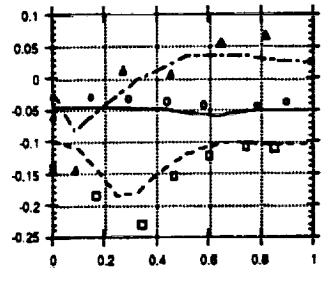

Piquet & Visonneau

Shen, Zhang & Cai

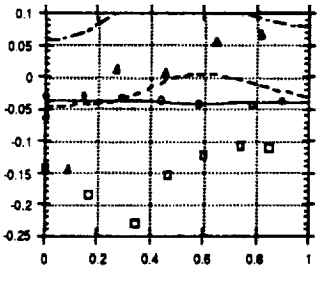

Tzabiras

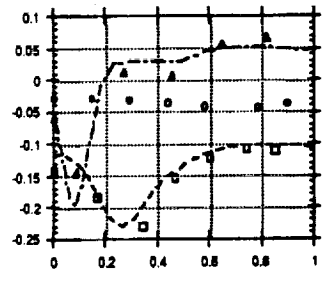

Zhou & Gao

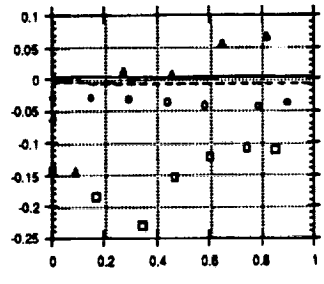

Zhu & Miyata

Legend:

exp calc

- c_p at x/L=0.646
- c_p at x/L=0.875
- c_p at x/L=0.942

3. Pressure distribution at three sections

Abdallah & Sotiropoulos

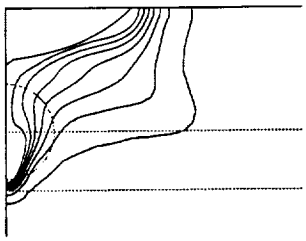

Broberg, Zhang, Larsson & Schöön

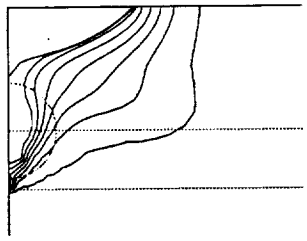

Bull, Watson & Musker

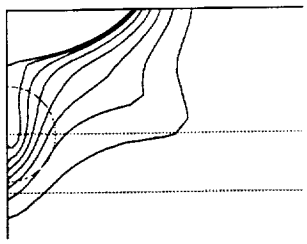

Caprino & Traverso

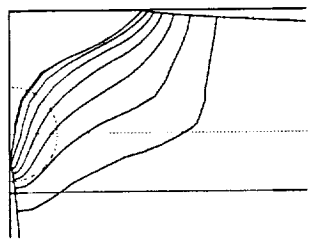

Gorski, Coleman, Haussling & Miller

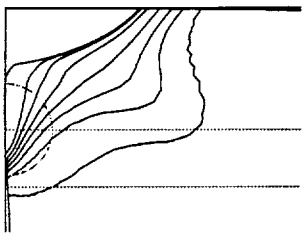

Hoekstra

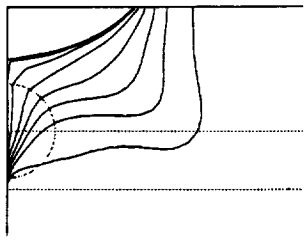

Hoffman &Chan

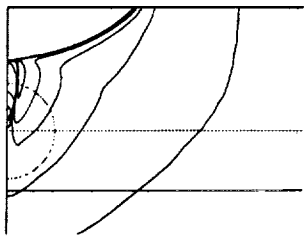

Ikehata & Liu

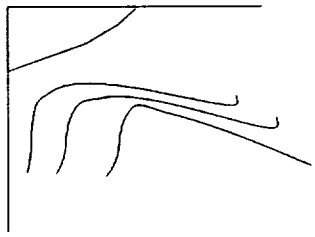

Kang & Oh

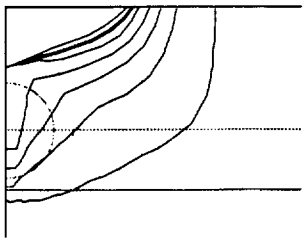

Kodama

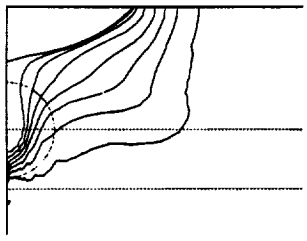

Kanevsky & Orlov

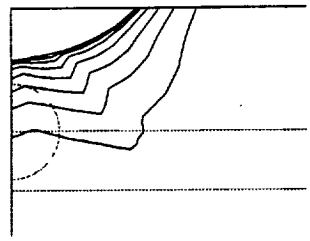

Majumdar, Zhu & Rodi

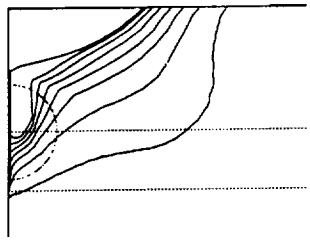

Masuko, Shirose & Abe

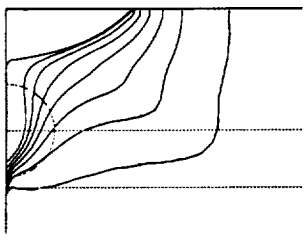

Patel, Ju & Lew

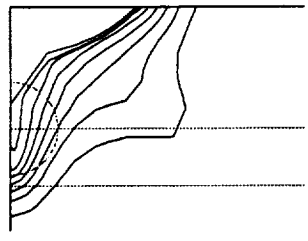

Piquet & Visonneau

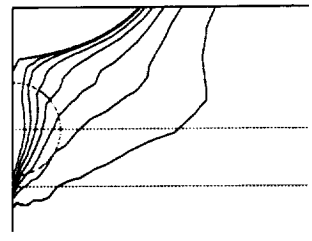

Shen, Zhang & Cai

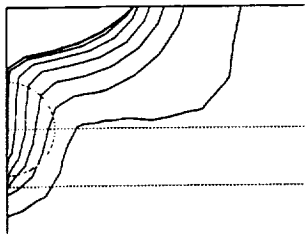

Tzabiras

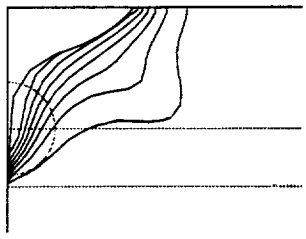

Zhou & Gao

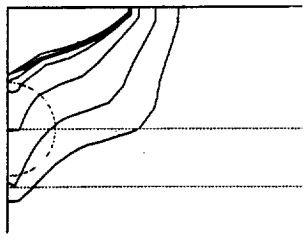

Zhu & Miyata

Experiment

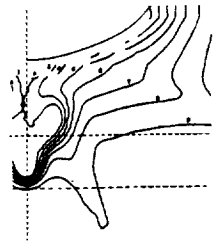

4. Axial velocity contours at the propeller plane X/L = 0.976 (U/U_∞ = 0.3, 0.4, 0.5, 0.6, 0.7, 0.8, 0.9)

Abdallah & Sotiropoulos

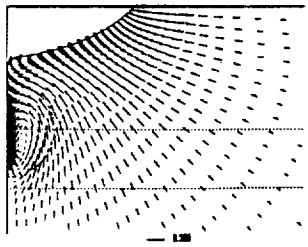

Broberg, Zhang, Larsson & Schöön

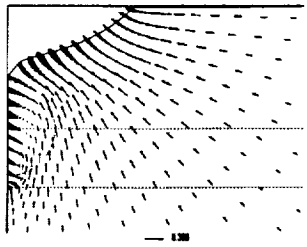

Bull, Watson & Musker

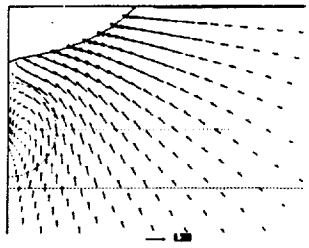

Caprino & Traverso

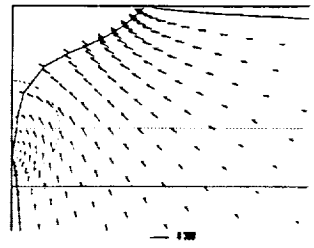

Gorski, Coleman, Haussling & Miller

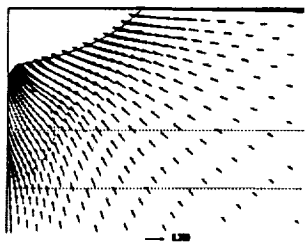

Hoekstra

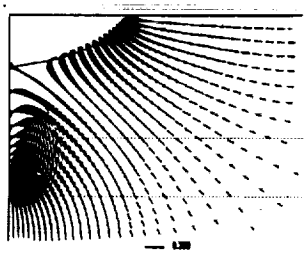

Hoffman &Chan

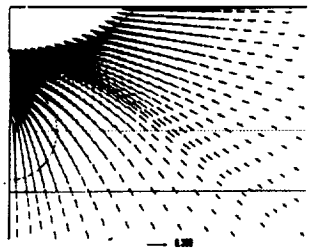

Ikehata & Liu

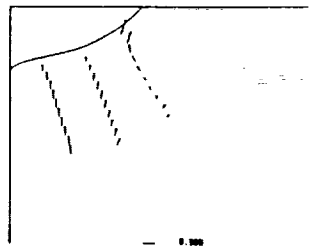

Kang & Oh

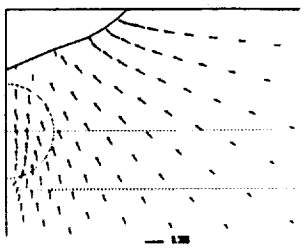

Kodama

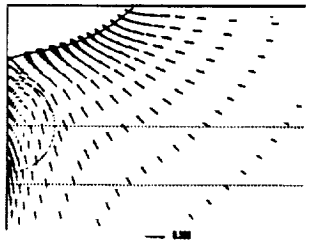

Kanevsky & Orlov

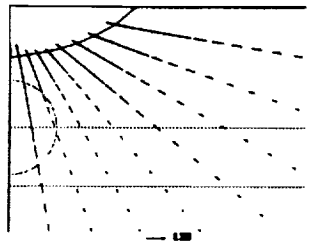

Majumdar, Zhu & Rodi

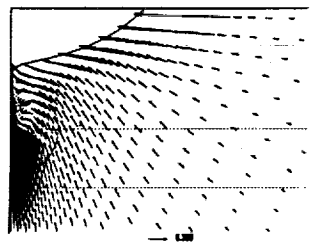

Masuko, Shirose & Abe

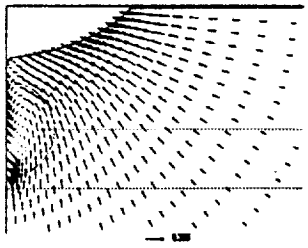

Patel, Ju & Lew

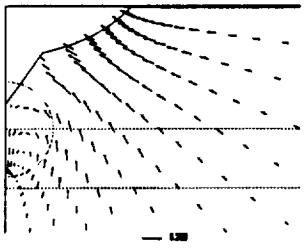

Piquet & Visonneau

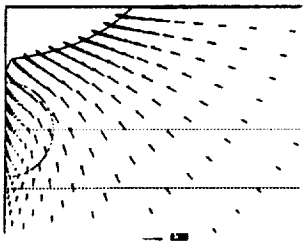

Shen, Zhang & Cai

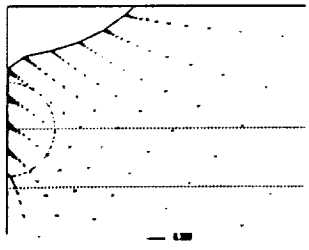

Tzabiras

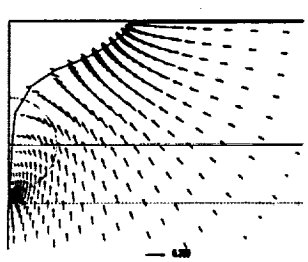

Zhou & Gao

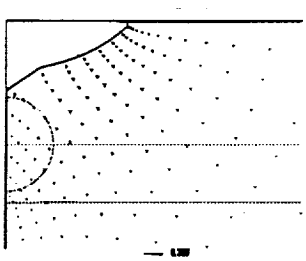

Zhu & Miyata

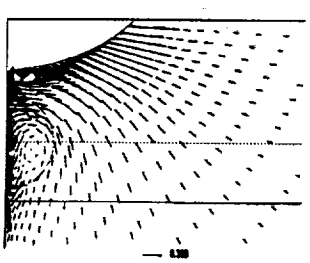

Experiment

Note velocity scale!

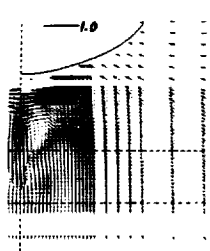

5. Cross-flow velocity vectors at the propeller plane X/L = 0.976

cross-flow vectors) at the propeller plane of Case I, see Figs. 3, 4 and 5. In these Figures the results of all 19 methods are included. Measured data are represented by symbols in Fig. 3, while the computed results are given as lines. In Fig. 4 iso-velocity contours corresponding to 0.3, 0.4, 0.5, 0.6, 0.7, 0.8 and 0.9 times the undisturbed velocity are given. For comparison the experimental data are shown in the lower right corner. Note the different scales for the computed and experimental cross-flow vectors in Fig. 5.

Before embarking on a more detailed analysis a comparison of the results presented at this Workshop with those obtained a decade ago for the SSPA-ITTC Workshop on Ship Boundary Layers[1] is quite revealing. Fig. 6 shows the axial velocity contours for the HSVA Tanker at X/L=0.942 presented at the previous Workshop. A comparison of these with the results shown in Fig. 4 provides an overview of the achievements of the past decade. It is clear that the earlier boundary layer methods have given way to those based on the Navier-Stokes equations. Only one such method was represented in 1980. At the present Workshop, only one boundary layer method was represented. The question is whether or not real progress has been achieved in the prediction of the flow. If the contours of axial velocity at the stern are used as the only measure of success, then we may conclude that progress has indeed been made. But, consider the following observation. Most calculations methods of the past did rather well at prediction of the boundary layer over the hull and failed only at the stern. Among the present methods, few, if any, predict the boundary layers with the same level of accuracy but continue to provide results for the flow over the stern and into the wake.

The girthwise pressure distributions of Fig. 3, will be considered section by section. First of all, we note that there are significant differences in the way different methods obtained the results at the check station, X/L = 0.646. As indicated in item A of Table 1 (Code H), seven methods performed calculations for the entire hull, starting upstream of it. Although the manner in which this was accomplished differed, their results at the check station reflect, to some extent, their resolution of the flow over the bow. Of the remaining methods, three started the calculations at the check station itself (see item D, Table 1) using the integral parameter information provided there. Note that no information on the crossflow at the check station was provided. The remaining methods started the solutions on the hull somewhere upstream of the check station and may have used the information provided to guide the selection of the upstream conditions. These differences among the methods must be taken into consideration when examining the results at the check station as well as further downstream.

In view of the foregoing, the results of four of the seven methods that calculated the flow over the entire hull are in remarkably good agreement with the data with respect to the girthwise pressure distribution at the first station. In fact, their predictions are as good as those of some of the methods that started the solutions on the hull. Methods that started the calculations on the hull show varying levels of agreement in the pressure distribution at the check station. The disagreement at the check station of methods that started at that station, or just upstream, are rather surprising. The reasons for this are not clear. Be that as it may, these differences should be borne in mind as comparisons are made further downstream.

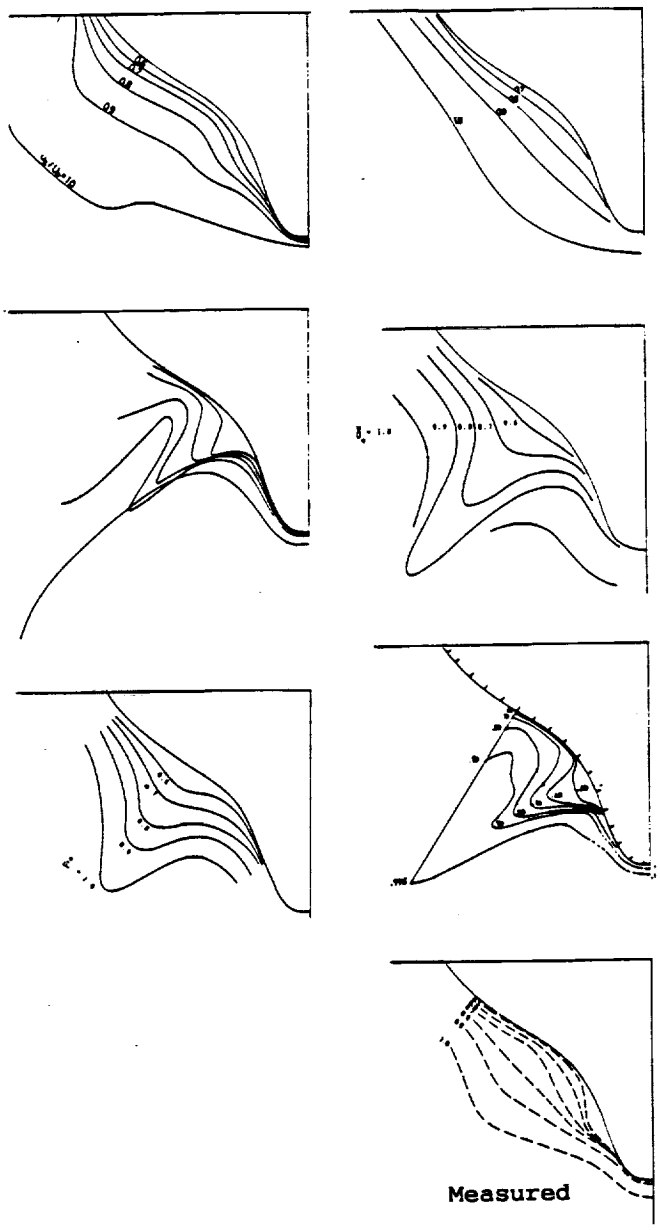

6. Axial velocity contours at X/L = 0.942, predicted in the 1980 Workshop[1].

At the next downstream section, X/L = 0.875, we see that the measured pressure distribution shows a decrease from the

keel, with a minimum c_p of about -0.24 around 30 percent of the girth, an increase up to about 70 percent of girth, followed by a near constant value of -0.11 around the waterline. It is clear from Fig. 3 that many methods reproduce this trend but, with one possible exception, fail to predict either the magnitude or the location of the pressure minimum.

At the last section, X/L = 0.942, the measurements indicate minimum cp at around 8 percent girth, much closer to the keel than at the previous station, and an increase followed by a constant pressure around the waterline. The calculations generally predict higher pressures throughout and all fail to capture the dip in pressure around 45 percent girth. The methods that did poorly at the previous station continue to yield poor results at this station also.

From the point of view of propeller design the most interesting results are those at the propeller plane, reported in Figs. 4 and 5. The propeller disk is indicated in these Figures, and it is seen that particularly in this area the results vary considerably between the different methods. For classification purposes it is possible to distinguish between three types of results, see Fig. 7.

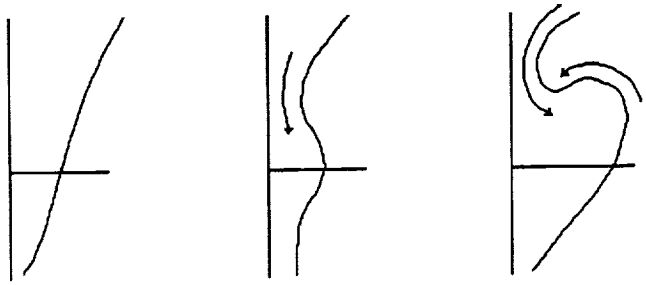

7. Different types of axial velocity contours at the propeller plane.

A. V-shaped contours

B. Contours with a bulge at or below the propeller center, indicating that part of the ship boundary layer has been displaced downwards by the longitudinal vortex hitting the propeller plane slightly above the propeller center (see Fig. 5).

C. Contours with a pronounced "hook" due to the action of a stronger vortex.

Obviously the measured wake is of type C with quite distinct hooks in the 0.3 and 0.4 contour curves.

Investigating the contours of Fig. 5 it is seen that only one method produced a wake of type C, but the results of this method outside the propeller disk, particularly near the waterline, look quite unrealistic. Four or five methods predicted a wake of type B, while the remaining ones produced A type wakes.

For a propeller designer this situation is unsatisfactory, since the wake distribution determines the variation in loading during one turn of the propeller, i.e. the vibratory forces. On the other hand, as was shown by one of the authors (Larsson) at a continued Workshop in Osaka in the fall of 1991, the mean value around the circle at all radii may still be well predicted, as may the mean value of the velocity in the entire propeller disk. This means that the pitch and its distribution on the blades might be reasonably well predicted using the calculated wakes of the 4-5 best methods.

The reason for the failure to predict hook-like velocity contours was discussed extensively during the Workshop. To structure the discussion it was divided into four main themes: grid generation, equations and boundary conditions, turbulence models and numerical method.

There appeared to be a general consensus that grid resolution was not a major cause of the differences between, on the one hand the methods themselves, and on the other hand the measurements. This opinion was substantiated by the fact that several computors had carried out grid independence studies with very small changes in the results. There was however a general feeling that the resolution of the transverse pressure gradient was too low near the bilge (region of high transverse curvature) on the afterbody. Since this is where the longitudinal vortex is generated, the lack of resolution could explain the too-weak vorticity in the wake predicted by most methods. An impression of the grids used can be obtained from Fig 5, although, for clarity, not all the grid points are shown for some methods.

As for the governing equations, a difference not reported in the questionnaire turned out to be the way in which the turbulence terms are considered. It became clear that only a few methods include all of the terms. Another difference in the governing equations (appearing from Table I) is that some methods use the partially-parabolic approximation, while others are fully elliptic. This difference was discussed, and it was concluded that no correlation could be found between the approximation level in this respect and the performance of the method, as judged by the results reported. Some participants had in fact computed Case I using both types of equations and found very small differences.

Different inlet boundary conditions are required depending on whether the computational domain starts on the hull or upstream of it, but in all cases the participants were free to match their solution to the measured data at X/L = 0.646. Large differences are, however, seen at this sta-

tion, indicating that this possibility was not exploited by most of the computors. Instead, the boundary layer at the inlet station, if on the hull, seems to have been estimated from flat-plate correlations. The methods starting upstream use uniform inlet flow. To avoid numerical problems a nonzero value of the eddy viscosity had to be applied right from the start. Values of 50 to 100 times the laminar viscosity were mentioned. No attempt was made to consider transition. The general feeling was that the inlet conditions did not significantly influence the results at the stations on the afterbody and in the wake. This conclusion had in fact been verified by some participants.

Some discussers expressed the opinion that the only way to resolve details of the flow close to the wall (such as limiting streamlines) is to abandon the wall law. The general opinion was, however, that it is difficult to see a large difference in performance between the methods using the wall law and the others. A better prediction of the wake contours would have been expected, and this was achieved by some of the non-wall law methods but not all. It was pointed out also that virtually the only way to compute the full scale case is to employ the wall law, since otherwise the innermost grid points have to be positioned extremely close to the surface, giving rise to problems with the cell aspect ratios (the non-dimensional distance from the surface, y/L, is about 250 times smaller for the full scale case for a given value of y+). The other boundary conditions were considered relatively unimportant for the problems at hand.

Different opinions on the general importance of turbulence modeling were expressed. It was argued that as experiments have indicated that the Reynolds stresses are very small in the major part of the viscous region near the stern, even an inviscid calculation might produce a reasonable result. Some participants reported on earlier computations for axisymmetric and three-dimensional bodies, where this approach had been tested with relatively good results. Obviously the inviscid region had to be restricted to the neighborhood of the stern.

A possible explanation for the failure to predict the correct wake contours might be the inability of the methods to resolve the pressure field accurately, i.e. to predict the transverse pressure gradients that are believed to produce the vortical flow structure. In this case, a number of numerical issues are involved, including the grid arrangement used (staggered versus regular) and the manner in which the pressure is calculated.

Conclusions

The Workshop clearly showed that great progress has been made during the 1980's in the development of methods for predicting the flow around the stern and in the near wake of ships. The boundary layer based approaches of the 1980 Workshop have given way to methods based on the Reynolds-Averaged Navier-Stokes equations, albeit using relatively simple turbulence models. While the former methods either broke down before, or predicted completely unrealistic results in the propeller plane, the new methods in general capture the gross features of the wake, such as the thin shear layer in the lower part and the piling-up of boundary layer low speed flow around half draught. In fact, the best methods of the Workshop predict the shape and location of the velocity contours in most of the propeller plane with reasonable accuracy. The results are however less satisfactory in the central part of the wake, i.e. inside the propeller disk. The bilge vortex, although weak, redistributes the low speed flow from the boundary layer in such a way that very uneven hook shaped velocity contours are created. This feature is missed to varying degrees by the different methods. Various reasons for this were discussed during the Workshop, but no definite answer could be given. One possible explanation is that the large velocity and pressure gradients in the bilge region are too inaccurately resolved in the grids employed.

There are no general differences in performance between methods based on zero equation turbulence models as compared to the two equation models. The disadvantages of the simpler models may be outweighed by the advantages of computing the flow all the way down to the surface. Two equation models are usually employed in combination with the wall law.

Although the new methods are superior to the old ones in predicting the wake, results from calculations starting upstream of the hull, or in front of the check station, indicate that the ability to predict the thin boundary layer has not been improved, rather the contrary. The likely reason for this is grid resolution. To save computer time very few grid points are located in the thin boundary layer on the forebody, where the much faster boundary layer methods may use grids with a very high resolution. This suggests a zonal approach where the expensive Navier-Stokes method is used in the stern and wake region while an efficient boundary layer method is used for the rest of the hull.

A final point to note is that most methods predicted, at least qualitatively, the differences between the two test cases.The computed cross flow for the second case is considerably larger in the propeller disk than for the first case, as the measurements have indicated, and the change in the contours of axial velocity also shows the right trend.

Acknowledgements

The authors are grateful to Dr J Kux and his group at the University of Hamburg for releasing their unpublished data for the second test case. Thanks are also extended to Professors G. Dyne, J. Piquet and W. Rodi, Mr M. Hoekstra and Mr D Humphreys for important technical discussions and advice, and to Mr B. Regnström for preparing all the graphs presented in the Proceedings.

The Workshop participation by V.C. Patel and IIHR was made possible by support from the Applied Hydromechanics Research program of the US Office of Naval Research under Grant N00014-89-J-1670, technically monitored by Mr J.A. Fein. The work at SSPA/FLOWTECH and CTH was sponsored by the Swedish National Board for Technical Development.

References

1 Larsson, L., (ed.) "SSPA-ITTC Workshop on Ship Boundary Layers 1980: Proceedings," SSPA, Goteborg, Sweden, Report No. 90, 1981.

2 Collatz, G., "Geosim Tests with a Model of Large Fullness," (in German) Forschungszentrum des Deutschen Shiffbaus, Report 28, Hamburg, 1972.

3 Hoffmann, H.P., "Investigation of the Three-Dimensional Turbulent Boundary Layer on a Double Model of a Ship in a Wind Tunnel," (in German) Inst. Schiffbau, Uni. Hamburg, Report 343, 1976.

4 Wieghardt, K. and Kux, J., "Nominal Wakes Based on Wind Tunnel Tests," (in German) *Jahrbuch der Schiffbautechnischen Gesellschaft (STG)*, 1980, Springer-Verlag, pp. 303-318.

5 Larsson, L., Patel, V.C. and Dyne, G., (ed.) "Ship Viscous Flow - Proceedings of the 1990 SSPA-CTH-IIHR Workshop", FLOWTECH, Gothenburg, Sweden, Research Report No 2, 1991.

6 Dyne, G., "A Study on the Scale Effect of Wake, Propeller Cavitation and Vibratory Pressure at the Hull of Two Tanker Models", *Trans SNAME*, 1974

7 Denker, J., Knaack, T. and Kux, J. "Experiments and Numerical Investigation of the HSVA2 Tanker (Second Test Case of the 1990 SSPA-CTH-IIHR Workshop), Inst. Schiffbau, Uni. Hamburg, Report 516, 1991.

Table I is found on the following 3 pages.

Table I

SUMMARY OF COMPUTATION METHODS
INFORMATION FROM RESPONSES TO QUESTIONNAIRE

A. OVERALL STRATEGY — Authors >>	AS	BZ LS	BW M	CT	GC HM	H	HC	IL	KO	K	KaO	MZ R	MS A	PJL	PV	SZ C	T	ZG	ZM
INDICATE whether you calculate the complete hull (by H), or only the stern and wake flow (by S)	S	S	S	H	S	S	S	H	S	H	H	H	H	S	S	S	S	S	H
GLOBAL (single method is used for entire flow) (G)	G	___	G	G	G	___	G	___	G	G	___	G	G	G	G	G	G	G	G
ZONAL (separate methods are used in different regions; matched or patched) (Z) ; [* indicates combinations]	___	Z	___	Z*	___	Z	___	Z	___	___	Z	___	___	___	___	___	___	___	___
Note: If ZONAL, complete the remainder for each viscous-flow region, carefully denoting the region to which the description applies. If a VISCOUS-INVISCID interaction method is used, indicate INTERACTION LAW: Displacement thickness (D); Surface and wake blowing or suction (S); Matching along a specified boundary outside the viscous layer (P); INVISCID METHOD used (I)	___	P,I	___	P,I*	___	P,I	___	P,I	___	___	?,I	___	___	___	___	___	___	___	___
B. EQUATIONS SOLVED																			
A PRIORI or DE FACTO APPROXIMATIONS None: Direct Simulation: no turbulence model (N); Large Eddy Simulation: NS equations with sub-grid model (L); Reynolds-averaged NS equations (R); RANS with grid-related approximations (e.g., nonorthogonal viscous terms neglected) (R-); Partially-parabolic RANS (longitudinal diffusion neglected; RANS with FLARE etc) (P); Thin-Layer RANS (only wall normal diffusion retained) (T); Boundary-layer equations (D: differential; I: integral)	R	R	R	R	R	P	R	I	R	R	P	R	R	R	R	Ra	R	P	L
VARIABLES Velocity and pressure (VP); Velocity and vorticity (VV); Stream function and vorticity (SV)	VP	VP	VP	VP	VP	VP	VP	I	VP	VP	VP	VP	VP	VP	VP	VP	VP	VP	VP
Choice of components of vector quantities [indicate by number(s)] Cartesian (1), cylindrical (2), other orthogonal (3), contravariant (4), covariant (5), grid-line oriented physical (6), mixed (M), other (7)	2	6	2	5	1	M	1	3	2	1	2	1	1	2	1	6	3	2	1
COORDINATES (see also GRID)																			
Nonorthogonal in all planes (3); Nonorthogonal in two planes (2); Nonorthogonal in one plane (1); Orthogonal in all planes (0); Other (finite elements, etc.) (A)	3	3	3	3	3	2	3	0	3	3	3	3	3	3	3	2	?	3	3
C. TURBULENCE MODEL																			
None (N); Sub-grid (SG); Algebraic eddy-viscosity or mixing-length (AL); One-equation (e.g., k); Two-equation (e.g., k,ε); Algebraic stress equations (AS); Reynolds stress equations (RS); Other (e.g., integral equations, I) Note: combinations indicated by two symbols (e.g., k ε, k)	AL	kε	kε	kε	AL	AL	kε k	I	kε	AL	kε	kε	kε	kε	kε k	kε	kε	kε	SG
Near-wall treatment: No-slip (NS); Law of the wall: with pressure-gradient (WP), without (W)	NS	WP	WP	W	NS	NS	NS	___	W	NS	?	W	W	WP	NS	W	W	W	NS
Number of turbulence-model equations solved	0	2	2	2	0	0	2	0	2	0	2	2	2	2	2	2	2	2	0
D. BOUNDARY AND INITIAL CONDITIONS																			
INITIAL (time = 0) From rest (O), uniform flow (1), potential flow (2), boundary layer solutions (4), other (5)	0	5	5	2 4	1	5	0	___	1	1	?	1	1	5	1	5	4	1	0
Variables determined in the above manner: Code - 0: p; 1: p, V; 2: V, k, ε; 3: p, V, k, ε	1	2	3	3	1	0	3	___	3	?	?	2	3	2	3	1	?	0	?
UPSTREAM Location (x = 0 is bow, x = L is stern), x/L =	.5	.5	.3	.2 -.51	.646	.646	.5	.05	.5	-.5	.1 .5	-.51	-.5	.3	.5	.5	.646	.5	-.5
Variables specified (e.g., C_f, δ, u, v, w, p, k, ε, v_t, ...) Code - 0: p; 1: integral parameters; 2: V; 3: V, k, ε	2	1,3	2,3	0,3	0,2	2	0,2	1	1,3	0,2	1	2,3	0,2	1	1	0,2	1	1	0,2
Conditions specified (e.g., uniform stream, 2D b.l. flow, ...) Code - 0: uniform stream; 1: inviscid flow; 2: 2DBL; 3: 3DBL	2	1,2	0,2	0 3	2	___	4	2	2	0	2,3	0	0	(3)	3	1,3	3	2	2
DOWNSTREAM Location, x/L =	1.8	2.0	5.	3.92	1.4	1.35	1.5	1.5	2.	1.5	<1	1.6	2.	4.5	2.	2.5	1.25	1.8	2.
Conditions specified Code - A: p_ξ, $\phi_\xi = 0$; A1: $p_\xi = 0$; B: p_ξ, $\phi_{\xi\xi} = 0$; C: V_{extrap}; D: p_{extrap};	B	B	B	A1	D,E	A1	A	___	A	?	___	A	A	B	A	A	E,A	A	?

WALL: No-slip (NS); wall function (WF)	NS	WF	WF	WF	NS	NS	NS	___	WF	NS	WF	WF	WF	WF	NS	WF	WF	WF	NS
WAKE CENTER Conditions Specified: Code - S: Symmetry {$U_n = 0$, $\partial(U_t, U_s, p,...)/\partial n = 0$)}	S	S	S	S	?	S	S	___	S	S	___	S	S	S	S	S	S	S	S
FREE SURFACE Double body, plane of symmetry (S), exact with fixed grid (G), exact with boundary-fitted grid (B), approximate (A, describe)	S	S	S	S	S	S	S	G	S	S	S	S	S	S	S	S	S	S	S
Conditions specified exact with boundary-fitted grid (B), approximate (A, describe)	S	S	S	S	S	S	S	___	S	S	S	S	S	S	S	S	S	S	S
FAR FIELD Location, R/L (or equivalent distance from axis) =	.5	.3	1.	1.	.375	.08	1.5	>.5	1.	1.	.7	.51	.5	1.	1.	.15	.1	.3	?.5
Tunnel/tank wall (T), uniform stream (U), inviscid flow (I)	U	I	U	U	U	I	U	I	U	U	I	U	U	U	U	I	I	?	?
Parameters specified: Code - B: $(p, U^1, U^2)_{inviscid}$; C_o: $U^1 = 1$, $\partial U^2/\partial n = 0$ C_1: $U^1 = 1$, $U^3 = 0$, $p = 0$; C_2: U^1, U^2, U^3, p;	___	B	C_1	C_2	C_2	B	?	B	C_1	C_1	B	S	C_1	C_1	C_o	B	B	___	___
Conditions specified: Code - A_1: $p_n = 0$, $\partial^2 U^i/\partial n^2 = 0$; A_2: $\partial(p, U^i)/\partial n = 0$; K_1: $\partial(k, \varepsilon)/\partial n = 0$; K_2: $(k, \varepsilon) = 0$; S: symmetry	A_1	K_1	K_1	A_2	___	___	___	___	K_2	___	___	S	___	K_1	K_1	K_1	___	A_2	A_2
E. GRID																			
TYPE Single block (SB) or multi-block (MB)?	SB	SB	SB	SB	MB	SB	SB	___	SB	SB	SB	SB	SB	SB	SB	SB	SB	SB	SB
Nonorthogonal everywhere (N), orthogonal in planes (P), orthogonal at some boundaries (B), orthogonal everywhere (O)	N	B	N	P	N	P	N	___	N	N	N	N	N	B	N	P	P	B	N
GENERATION METHOD Analytic (A), numerical (N), algebraic (L)	N	N	N	N	L	A,N	A,L	___	N	N	N	N,L	N	N	N	L	A	N	N,L
Elliptic (E), hyperbolic (H), parabolic (P), transfinite (T), conformal (C), geometrical (G)	E	E	E	E	T	C	C,T	___	E	G	?	T	E	E	E	G	C	E	E
3D (3), 2D plane by plane (2), other (1)	2	3	2	3	3	2	2	___	3	3	3	3	3	3	3	3	2	3	3
Post-generation smoothing? yes (Y), no (N)	N	N	N	Y	N	N	N	___	N	Y	N	N	Y	N	N	Y	N	N	Y
CONTROL Adaptive? yes (Y), no (N)	N	N	N	N	N	N	N	___	N	N	___	N	___	N	N	N	___	N	N
Control from boundaries (B), from inside the domain (D)	B	B	B	D	B	___	___	___	B	___	___	D	___	D	___	D	B	B,D	___
F. NUMERICAL METHOD																			
GENERAL CLASSIFICATION Finite-element (FE), finite-difference (FD), finite-volume (FV), Spectral (S), Integral (I), mixed (M), Other (O)	FD	M	M	FV	FV	FD	FV	I	FV	FD	FV	FV	FV	M	M	FV	FV	FD	FV
	NO FINITE-ELEMENT METHOD REPRESENTED																		
DISCRETIZATION Finite-difference, regular or collocated grid (R); finite-difference, staggered grid (T); finite volume, regular grid (V); finite-volume, staggered grid (S); finite element (L); hybrid (H) & other (O), specify	R	S	S	S	V	R	R	___	S	R	V	R,V	S	S	R	S	S	T	S
DIFFERENCING OF CONVECTIVE TERMS Centered (C); upwind, standard (U); upwind, skewed (K); rotated (A); explicit artificial viscosity (D); hybrid, specify (H); other, specify (O) Code - finite-analytic (FA)	U	FA	FA	U	U	O	U,D	___	C,U	C,D	O	H	C,U	FA	O	H	U,C	U	H
FORMAL ORDER OF ACCURACY (Convective terms) First (1); second (2); third (3); fourth (4); mixed (M); other (O)	2	M	M	M	3	2	2	___	M	2	1	1	1,2	1,2	1,2	M	1,2	2	3
FORMALLY CONSERVED QUANTITIES Mass (Q); mass and momentum (M); mass, momentum, kinetic energy (J); mass, momentum, total energy (W); other (O) Note: There is some confusion here about conserved quantities	M	Q	J	J	M	M	M	M	J	M	M	M	M	J	Q	M	J	M	M
LINEARIZATION: Picard (P); Newton (N); Quasi-Newton (Q); Other (O)	___	___	P	___	N	N	N	___	O	N	P	P	___	O	Q	___	___	N	N
PRESSURE-VELOCITY COUPLING Fully-coupled solutions: direct method (D); penalty method (P); compressible-flow code used at low Mach number (C); artificial compressibility (A); other (O)	O	___	___	___	A	O	___	___	___	A	___	___	___	___	___	___	___	___	?

Segregated: Poisson equation, e.g., capacitance techniques (P); pressure-correction technique, e.g., SIMPLE, SIMPLER, SIMPLEC, PISO, saddle-point method, preconditioning (C, list); other (e.g., boundary-layer type code) describe (O) Code - S_1: SIMPLE; S_2: SIMPLER; S_3: SIMPLEST; S_4: SIMPLEC; P: PISO	---	S_2	S_2	S_3	---	---	P	---	S_1	---	S_1	S_1	S_1	S_2	P	S_1	S_1	S_4	?
ACCELERATION OF ITERATIVE SOLUTIONS If you distinguish more than one iteration process in your method, classify them and specify the following for each of them: Under-relaxation (U); over-relaxation (R); grid sequencing (G); (U) on p only; multi-grid (M); additive terms (e.g., quasi-time dependent, fixed or variable time step) (A); conjugate gradient methods (C); other, describe (O)	U A	A	R	U	O	G,U A	C	---	U	---	---	U	U	A	A	U	U	U	U
STRATEGY Explicit (E); implicit (I); semi-implicit (S); fractional step (F); other (e.g., optimal control, Newton-Raphson), describe (O)	E	I	S	---	I	I	S	---	I	I	I	I	S	I	I	I	I	S	E,S
TACTICS Point substitution (P); line substitution (L); direct matrix inversion (M); Split (ADI-like); incomplete LU decomposition (D); other, describe (O)	P	L	L	O	D	P,D	D	---	L	Split	L	D	P	L	D	L	P,L	L	P
G. COMPUTATIONS Computer used, list Code - S_y: CRAY YMP; S_x: CRAY XMP; S_2: CRAY 2; S_{f2}: FACOM VP400; S_{f1}: FACOM VP50 M_d: DEC 2100; M_f: FPS 264; M_v: MICROVAX 3800;M_a: Apollo 10000; M_s: SUN 4WS; M_{st}: STELLAS WS; M_b: BESM6; M_i: IBM 3031; M_{sp}: SPARC 330; (Note: S for super; M for other)	S_y	M_d	M_f	M_v	S_x	S_x	M_a	---	M_s	M_{st}	M_b	S_{f2}	S_{f1}	S_y	S_2	M_i	M_{sp}	M_i	M_{st}
Number of grid points used in axial and transverse directions:	57 41 33	60 33 25	93 40 21	63 16 25	65 33 49	113 55 35	92 86 32		58 25 16	81 27 31	50 10 20	124 44 32	133 25 29	50 30 15	80 40 21	36 20 12	45 29 62	80 15 20	120 30 30
Total number of grid points, thousands (K)	79	49	78	25	105	218	253		23	68	10	175	96	23	67	8	81	24	108
For above grid, storage utilized (MW: megawords MB: megabytes)	MW 2.4 MB ---	--- 6	--- 24	--- 11	3 ---	1 ---	--- ---	--- ---	--- 8	--- 20	 ---	63 ---	30 ---	1.8 ---	12 ---	--- 0.2	--- ---	--- 0.4	--- 56
For above grid, cpu time: m: min; h: hours; d: days	90m	2h	30h	10h	9h	80m	20h	---	3h	50h	30h	11m	2h	10m	4h	5h	---	3h	5d
For above grid, number of iterations or time steps required for convergence, in thousands (K)	4.	.04	1.6	.3	2.5	.035	1.	---	.13	5.	---	.1	.4	.16	.3	.04	.06	.06	20.
Convergence criteria employed Code - NE: no explicit criterion; O: other A: 1 $\Delta p < 5\,10^{-3}$; 2 $5\,10^{-4}$; 3 10^{-4}; 4 B: $\Sigma S <$ 10^{-3}; $5\,10^{-4}$; 10^{-5}; $5\,10^{-5}$ C: $\Delta u < 10^{-4}$	A_3C	NE	---	NE	NE	A_1	B_1	---	B_1	NE	---	B_2	B_4	NE	A_3C	C	B_3	A_2	A_3
Approximate cpu per iteration per grid point, in 10^{-5} secs	2	500	92	---	11.4	---	29	---	388	50	---	3.9	13	16	50	2780	615	625	20
Maximum grid that can be accommodated on the computer in thousands (K)	---	---	300	---	120	---	---	---	---	123	---	705	500	112	1000	---	---	32	110
Number of grid points used in the region $0.65 < X/L < 1.0$, $n^+ > 100$, $n/L < 0.1$ axial radial girth	 --- ---	33 20 25	--- ---	--- ---	--- ---	--- ---	--- ---	--- ---	--- ---	--- ---	--- ---	--- ---	--- ---	--- ---	30 20 21	--- ---	--- ---	--- ---	--- ---
Total number of grid points in the above region, thousands (K)	---	16.5	---	---	---	---	---	---	---	---	---	---	---	---	12.6	---	---	---	---

AUTHORS CODE

AS:	Sotiropoulos & Abdallah, Uni. Cincinnati, USA
BZLS:	Broberg, Zhang, Larsson & Schoon, Flowtech, Sweden
BWM:	Bull, Watson & Musker, ARE-Haslar, U.K.
CT:	Caprino & Traverso, CETENA, Italy
GCHM:	Gorski, Coleman, Haussling & Miller, DTRC, USA
H:	Hoekstra, MARIN, The Netherlands
HC:	Hoffman & Chan, ARL, Penn State Uni. & Rockwell, USA
IL:	Ikehata & Liu, Yokohama Nat. Uni., Japan
KO:	Kang & Oh, Seoul Nat. Uni., & Kyungnam Uni., Korea
K:	Kodama, Ship Res. Inst., Japan
KaO:	Kanevsky & Orlov, Krylov, USSR
MZR:	Majumdar, Zhu & Rodi, NAL, India & Uni. Karlsruhe, Germany
MSA:	Masuko, Shirose & Abe, IHI, Japan
PJL:	Patel, Ju & Lew, IJHR, Uni. Iowa, USA & Daewoo, Korea
PV:	Piquet & Visonneau, ENSM Nantes, France
SZC:	Shen, Zhang & Cai, MARIC, China
T:	Tzabiras, Nat. Tech. Uni., Greece
ZG:	Zhou & Gao, CSSRC, China
ZM:	Zhu & Miyata, Uni. Tokyo, Japan